



**HAL**  
open science

## Investigation on the properties of linear PLA-poloxamer and star PLA-poloxamine copolymers for temporary biomedical applications.

Adrien Leroy, Coline Pinese, Claire Bony, Xavier Garric, Danièle Noël, Benjamin Nottelet, Jean Coudane

### ► To cite this version:

Adrien Leroy, Coline Pinese, Claire Bony, Xavier Garric, Danièle Noël, et al.. Investigation on the properties of linear PLA-poloxamer and star PLA-poloxamine copolymers for temporary biomedical applications.. Materials Science and Engineering: C, 2013, 33 (7), pp.4133-4139. 10.1016/j.msec.2013.06.001 . hal-00967461

**HAL Id: hal-00967461**

**<https://hal.science/hal-00967461v1>**

Submitted on 22 Jan 2024

**HAL** is a multi-disciplinary open access archive for the deposit and dissemination of scientific research documents, whether they are published or not. The documents may come from teaching and research institutions in France or abroad, or from public or private research centers.

L'archive ouverte pluridisciplinaire **HAL**, est destinée au dépôt et à la diffusion de documents scientifiques de niveau recherche, publiés ou non, émanant des établissements d'enseignement et de recherche français ou étrangers, des laboratoires publics ou privés.



Distributed under a Creative Commons Attribution - NonCommercial - NoDerivatives 4.0 International License

# Investigation on the properties of linear PLA-ploxamer and star PLA-ploxamine copolymers for temporary biomedical applications

Adrien Leroy<sup>a,b</sup>, Coline Pinese<sup>a</sup>, Claire Bony<sup>b</sup>, Xavier Garric<sup>a</sup>, Danièle Noël<sup>b</sup>, Benjamin Nottelet<sup>a,\*</sup>, Jean Coudane<sup>a</sup>

<sup>a</sup> Institut des Biomolécules Max Mousseron (IBMM), UMR CNRS 5247, University of Montpellier 1, University of Montpellier 2–Faculty of Pharmacy, 15 Av. C. Flahault, Montpellier, 34093, France

<sup>b</sup> INSERM U844, Hôpital Saint-Eloi, 80 Av. Augustin Fliche, 34091 Montpellier Cedex 5, France

## A B S T R A C T

The objective of this work was to develop and study new biodegradable thermoplastics with improved mechanical properties for potential use as temporary implantable biomaterials. Linear poloxamer and star-shaped poloxamine have been used as macroinitiators for the ring-opening polymerization (ROP) of lactide to yield high molecular weight PLA-based thermoplastic block copolymers. The influence of the nature of the macroinitiator, PLA crystallinity and initial molecular weight on the copolymers properties was investigated by performing a 7-week degradation test in PBS. The evaluation of water uptakes and molecular weights during the degradation pointed out an early hydrolytic degradation of the 100-kg·mol<sup>-1</sup> copolymers compared to the 200-kg·mol<sup>-1</sup> ones (molecular weight decrease of ca. 40% and 20%, respectively). A dramatic loss of tensile mechanical properties was also observed for the 100-kg·mol<sup>-1</sup> copolymers, whereas the 200-kg·mol<sup>-1</sup> copolymers showed stable or even slightly improved properties with Young's moduli around 500 MPa and yield strains around 3% to 4%. Finally, the cytocompatibility of the more stable 200 kg·mol<sup>-1</sup> copolymers was confirmed by murine mesenchymal stem cells (MSCs) culture.

## 1. Introduction

Synthetic aliphatic polyesters derived from lactide (LA), glycolide (GA),  $\epsilon$ -caprolactone (CL) and their copolymers are among the most widely used degradable polymeric biomaterials for medical applications including implantable devices [1], drug delivery systems [2–4] or tissue engineering materials [5–7]. Although particularly popular thanks to its good biocompatibility, poly(lactide) (PLA) does not meet optimal properties to replace soft tissues like ligaments, tendons, cartilage or blood vessels [8–10].

Different strategies are currently used to modify PLA and obtain temporary implantable biomaterials with improved mechanical properties. Cross-linking is one of the most studied techniques [11–15] as it leads to the formation of structures similar to vulcanized rubbers. One of the drawbacks of these materials is that they cannot be remolded by heating or solvent casting because of their cross-linked structure, which makes them difficult to design with complex shapes. Another interesting way is the synthesis of thermoplastic elastomers (TPE), which involves two polymers: a first one is acting as a rigid and hard segment responsible for mechanical strength and a second flexible and soft segment to yield elasticity. Several groups have prepared such materials by associating rigid PLA blocks with more flexible segments like

poly( $\epsilon$ -caprolactone) (PCL) [16,17], polyethylene glycol (PEG) [18] or poly(trimethylene carbonate) (PTMC) [19,20], or by chain extension [21,22]. However, it remains difficult to obtain biocompatible and biodegradable thermoplastic materials with high mechanical strength. In particular, most of the above-mentioned polymers exhibit low Young's moduli (in the range 5 to 70 MPa) or low yield stress values (in the range 1–10 MPa) [16,17,20].

The objective of this work is therefore to propose alternative degradable PLA block and star copolymers with improved mechanical properties to be used as temporary implantable materials. Our group being involved in the synthesis and study of PLA-PEG block copolymers for many years [18,23,24], we were interested in evaluating high molecular weight PLA-ploxamer-PLA and PLA-ploxamine-PLA as thermoplastic and biodegradable block copolymers. As far as we know, such copolymers have mainly been used as nanoparticles, microspheres or hydrogels for drug delivery applications and not as materials for biomedical substrates. In association with semi-crystalline PLA, which is biocompatible and biodegradable but has too high mechanical properties when used alone, linear poloxamer and 4-arm poloxamine have been chosen as macroinitiators to confer some elasticity to the material thanks to their structure containing PEG flexible blocks. Besides, four-arm poloxamine should have the ability to generate chain entanglements and physical cross-linking in the polymer network. Associated with different lengths of PLA blocks, these polyether soft segments can change the mechanical properties and the hydrophilic-hydrophobic balance in order to

\* Corresponding author. Tel.: +33 411 759 697.

E-mail address: benjamin.nottelet@univ-montp1.fr (B. Nottelet).

modulate the degradation rate. Finally, keeping *in vivo* implantation in mind, we have evaluated the influence of some key parameters like the nature of the central block, the molecular weight and the PLA crystallinity on the materials properties during degradation. A particular attention has been paid to the evolution of molecular weight, thermal properties and mechanical properties. The cytocompatibility of the more promising candidates was finally assessed by studying the viability of murine mesenchymal stem cells (MSCs).

## 2. Materials and methods

### 2.1. Materials

Poloxamine (Tetronic® 1107; 15,000 g/mol) was purchased from BASF (Levallois Perret, France). Poloxamer (Pluronic® F-127; 12,600 g/mol), tin(II) 2-ethylhexanoate (Sn(Oct)<sub>2</sub>, 95%), dichloromethane (DCM), diethyl ether and tetrahydrofuran (THF) were purchased from Sigma-Aldrich (St-Quentin Fallavier, France). D-Lactide (D-LA), L-lactide (L-LA) and D,L-lactide (D,L-LA) were purchased from Purac (Lyon, France). PrestoBlue™, Dulbecco's modified Eagle's medium (DMEM/F-12), phosphate-buffered saline (PBS), sterile Dulbecco's phosphate-buffered saline (DBPS), fetal bovine serum (FBS), penicillin, streptomycin and glutamine were purchased from Invitrogen (Cergy Pontoise, France). BD Falcon™ Tissue Culture Polystyrene (TCPS) 24-well plates were purchased from Becton Dickinson (Le Pont de Claix, France) and Viton® O-rings from Radiospares (Beauvais, France). All chemicals and solvents were used without purification.

### 2.2. Characterizations

The number average molecular weight ( $M_n$ ) and the polydispersity (PD) of the polymers were determined by size exclusion chromatography (SEC) using a Viscotek GPCMax autosampler system fitted two Viscotek LT5000L mixed medium columns (300 × 7.8 mm), a Viscotek VE 3580 RI detector. The mobile phase was THF at 1 mL/min flow and 30 °C. Typically, the polymer (20 mg) was dissolved in THF (2 mL), and the resulting solution was filtered through a 0.45-μm Millipore filter before injection of 20 μL of filtered solution.  $M_n$  was expressed according to calibration using polystyrene standards.

<sup>1</sup>H NMR spectra were recorded at room temperature using an AMX300 Bruker spectrometer operating at 300 MHz. Deuterated chloroform was used as solvent, chemical shifts were expressed in ppm with respect to tetramethylsilane (TMS). Differential scanning calorimetry (DSC) measurements were carried out under nitrogen on a Perkin Elmer Instrument DSC 6000 Thermal Analyzer. Samples were submitted to a first heating scan to 200 °C followed by a cooling (10 °C.min<sup>-1</sup> from 200 °C to 100 °C, and 7 °C.min<sup>-1</sup> from 100 °C to -30 °C) and a second heating scan to 200 °C (10 °C.min<sup>-1</sup>). Glass transition temperature ( $T_g$ ), crystallization temperature ( $T_c$ ), melting temperature ( $T_m$ ) and melting enthalpy ( $\Delta H_m$ ) were measured on the second heating ramp.

### 2.3. Copolymers syntheses

PLA-Pluronic-PLA and PLA-Tetronic-PLA block copolymers were synthesized following a procedure previously described by our group [25]. Typically, predetermined amounts of LA and Pluronic or Tetronic were introduced into a flask, and Sn(Oct)<sub>2</sub> (0.1 molar % with respect to LA units) was then added. After degassing, the flask was sealed under vacuum, and polymerization was allowed to proceed at 110 °C. After 5 days, the copolymer was recovered by dissolution in DCM and precipitation in cold diethyl ether. Finally, the product was dried under reduced pressure to constant mass. The copolymers were obtained with an average yield of 86% (43 g).

<sup>1</sup>H NMR: (300 MHz; CDCl<sub>3</sub>):  $\delta$  (ppm) = 5.1 (q, 1H, CO-CH(CH<sub>3</sub>)-O), 3.6 (s, 4H, CH<sub>2</sub>-CH<sub>2</sub>-O), 3.5 (m, 2H, CH(CH<sub>3</sub>)-CH<sub>2</sub>-O), 3.4 (m, 1H,

CH(CH<sub>3</sub>)-CH<sub>2</sub>-O), 1.5 (m, 3H, CO-CH(CH<sub>3</sub>)-O), 1.1 (m, 3H, CH(CH<sub>3</sub>)-CH<sub>2</sub>-O).

Polymerization degree of PLA blocks and molecular weight of the synthesized triblock copolymers were calculated using the following equations.

$$DP_{PLA} = DP_{PEO}/(EO/LA) \quad (1)$$

For PLA-Pluronic-PLA copolymers:

$$M_n = 2 \times (DP_{PLA} \times 72) + M_n \text{ Pluronic} \quad (2)$$

For PLA-Tetronic-PLA copolymers:

$$M_n = 4 \times (DP_{PLA} \times 72) + M_n \text{ Tetronic} \quad (3)$$

where EO/LA is the ratio of ethylene oxide and lactyl units and PO/LA is the ratio of propylene oxide and lactyl units calculated from <sup>1</sup>H NMR spectra.

### 2.4. Tensile tests

Sample plates were prepared by compression of the polymer in stainless steel mould for 10 min at 200 °C and 8 tons using a Carver press (4120). For tensile mechanical tests, plates (30 × 10 × 0.5 mm) were analyzed at 37 °C in an Instron 4444 at a crosshead speed rate of 5 mm/min and each sample being loaded to failure. Each sample was analyzed in triplicate and Young's modulus ( $E$ , MPa), stress at failure ( $\sigma_f$ , MPa), strain at failure ( $\epsilon_f$ , %), yield stress ( $\sigma_y$ , MPa) and yield strain ( $\epsilon_y$ , %) were expressed as the mean value of the three measurements.  $E$  was calculated using the initial linear portion of the stress/strain curves.

### 2.5. Degradation tests

Sample plates were prepared by compression molding as previously described. Samples were cut (30 × 10 × 0.5 mm), precisely weighed (initial weight  $W_i$ ) and were then placed in 8 mL of PBS (pH 7.4) at constant temperature (37 °C) under stirring. At scheduled time points, samples were removed from PBS, weighed (hydrated weight  $W_h$ ), and their tensile mechanical properties were evaluated. After drying to constant mass, they were weighed (dry weight  $W_d$ ). Water uptake and weight loss of the samples were then calculated from the following equations.

$$\text{Water uptake(\%)} = 100 \times (W_h - W_d) / W_d \quad (4)$$

$$\text{Weight loss(\%)} = 100 \times (W_i - W_d) / W_i \quad (5)$$

Molecular weights and PD were determined by GPC. Molecular weights were also determined by <sup>1</sup>H NMR spectroscopy. Thermal properties were measured by DSC.

### 2.6. Cytocompatibility

Murine mesenchymal stromal cells C3H10T1/2 (designated C3 cells or C3 MSCs thereafter) were used to assess the *in vitro* cytocompatibility of the materials. C3 cells were cultured in proliferative medium composed of DMEM/F-12 without phenol red supplemented with 10% FBS, penicillin (100 U/mL), streptomycin (100 μg/mL) and glutamine (2 mM). Sample disks were cut (ø 15 mm) from copolymer films and disinfected in ethanol for 30 min before immersion in a solution of sterile PBS containing penicillin and streptomycin (1 mg/mL) and incubation for 48 h at 37 °C. Disks were then rinsed 2 times with sterile PBS before soaking for 12 h in sterile PBS. After disinfection, disks were placed in TCPS 24-well plates, and non-cytotoxic Viton® O-rings [26,27] were used to maintain the samples on the bottom of the wells and avoid cells growing on TCPS underneath the samples. Disks and empty TCPS

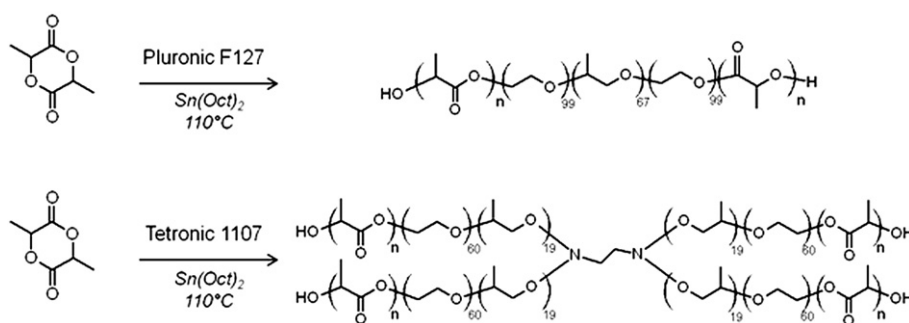


Fig. 1. General synthesis scheme of copolymers.

wells (positive control) were finally seeded with  $10^3$  C3 cells, which were then maintained in proliferative medium. Viability was evaluated after 2, 4 and 7 days using PrestoBlue assay, a cell-permeable resazurin-based viability reagent that reflects the number of living cells present on a surface at a given time point. At scheduled time points, proliferative medium was removed and replaced by 1 mL of fresh medium containing 10% of PrestoBlue. After 2 h of incubation at 37 °C, 200  $\mu$ L of supernatant was taken from each well and analyzed for UV absorbance at 570 nm (as the experimental wavelength) and 595 nm (as the normalization wavelength) with a Thermo Scientific Multiscan FC microplate photometer. Values and standard deviations correspond to separate experiments done in triplicate. Homogeneity of variances was checked using Bartlett's test, and one-way ANOVA was applied to determine the statistical significance for multiple comparisons (a level of  $p < 0.05$  was considered statistically significant).

Cell adhesion and proliferation were also assessed using PromoKine Live/Dead cell staining kit (PromoCell GmbH, Heidelberg, Germany). After culture in proliferative medium,  $10^3$  cells were seeded on disinfected polymer disks ( $\varnothing$  15 mm) maintained with O-rings on the bottom of TCPS 24-well plates. After 7 days, proliferative medium was removed and disks were rinsed 3 times with sterile PBS to eliminate non-adherent cells. C3 cells were then incubated in the presence of live/dead staining solution (2  $\mu$ M Calcein-AM and 1.5  $\mu$ M propidium iodide) at 37 °C for 15 min and fixed with 3.7% paraformaldehyde for 10 min. Cells were observed under a Leica TCS SP5 X confocal microscope (Leica Microsystems GmbH, Wetzlar, Germany).

### 3. Results and discussion

#### 3.1. Syntheses

With the aim of providing new degradable copolymers with original mechanical and degradation properties that are compatible with cell culture and tissue reconstruction, we took interest in copolymerizing bioresorbable and biocompatible thermoplastic materials combining PLA segments with Pluronic and Tetrionic. One advantage of this strategy is the possibility to modulate the material properties as a function of some parameters controlled by the copolymers design: composition and architecture of the central block, molecular weight, glass transition temperature ( $T_g$ ), hydrophilic–hydrophobic balance and crystallinity.

In first place, we have evaluated the influence of crystallinity on the copolymers mechanical properties by synthesizing copolymers with PLA<sub>50</sub>, PLA<sub>70</sub> and PLA<sub>94</sub>. This preliminary study (Fig. S1) pointed out as expected that copolymers containing PLA<sub>94</sub> had much better mechanical properties compared to PLA<sub>50</sub> and PLA<sub>70</sub>, especially after immersion in PBS. This observation led us to focus afterwards on copolymers with highly crystalline PLA blocks.

Following this preliminary study, six different copolymers were synthesized (Fig. 1). The influence of some macromolecular parameters on the *in vitro* degradation was studied. These parameters included the nature of the central block (Pluronic F127 or Tetrionic 1107), the crystallinity of the PLA blocks, which was controlled thanks to the copolymerization of defined amounts of D-LA and L-LA (PLA<sub>94</sub> or PLA<sub>96</sub>), and the global

Table 1  
Copolymers properties.

Copolymer	Composition	L-LA	D,L-LA	Initiator	$M_n$ ( $\text{kg}\cdot\text{mol}^{-1}$ )		$\bar{D}$	$T_g$	$T_m$	$\Delta H_m$
		(wt%)	(wt%)		(wt%)	NMR				
94P100	PLA <sub>94</sub> Pluronic 100 $\text{kg}\cdot\text{mol}^{-1}$	76.9	10.5	12.6	123.3	65.0	1.6	34.4	141.4	12.4
96P100	PLA <sub>96</sub> Pluronic 100 $\text{kg}\cdot\text{mol}^{-1}$	80.4	7.0	12.6	116.4	57.7	1.7	35.4	156.4	16.2
94 T100	PLA <sub>94</sub> Tetrionic 100 $\text{kg}\cdot\text{mol}^{-1}$	74.8	10.2	15	115.1	60.3	1.3	34.3	141.8	12.6
94P200	PLA <sub>94</sub> Pluronic 200 $\text{kg}\cdot\text{mol}^{-1}$	82.5	11.2	6.3	223.0	114.0	1.6	53.8	145.4	19.9
96P200	PLA <sub>96</sub> Pluronic 200 $\text{kg}\cdot\text{mol}^{-1}$	86.2	7.5	6.3	222.6	89.0	1.7	58.1	155.6	25.1
94 T200	PLA <sub>94</sub> Tetrionic 200 $\text{kg}\cdot\text{mol}^{-1}$	81.4	11.1	7.5	240.4	93.3	1.6	43.9	147.8	10.5

molecular weight of the copolymers ( $100 \text{ kg}\cdot\text{mol}^{-1}$  or  $200 \text{ kg}\cdot\text{mol}^{-1}$ ). Copolymers properties are summarized in Table 1.

Molecular weights of the copolymers were firstly determined by  $^1\text{H}$  NMR spectroscopy, thanks to Eqs. (1) to (3). Results were close to theoretical values, although a little higher. On the opposite, SEC analyses gave molecular weight values about two times lower than those calculated by NMR. This difference is explained by the use of polystyrene standards for SEC calibration causing inaccurate measurements with aliphatic polyesters [28,29]. Moreover, the amphiphilic nature of the copolymers can modify their hydrodynamic volume and increase their retention time, giving underestimated results. Molecular weights calculated from  $^1\text{H}$  NMR spectra are therefore more accurate since only copolymers but no PLA homopolymers were formed during the ROP as confirmed by the monomodal chromatograms obtained by SEC analyses and the spectra obtained by DOSY analyses (Fig. S2). As a consequence, values deduced from  $^1\text{H}$  NMR analyses can be considered as sound.

DSC analyses of the copolymers mainly showed an increase of  $T_g$  and  $T_m$  with the crystallinity of PLA blocks and molecular weight. In copolymers containing Pluronic, the molecular weight increase resulted in an increase of  $\Delta H_m$  and therefore of crystallinity. This was not observed for the Tetric-based copolymers, because the star structure probably hinders crystallization. Regarding  $T_g$  values that are of interest when considering implantation, it is remarkable that increasing the molecular weight of copolymers from  $100$  to  $200 \text{ kg}\cdot\text{mol}^{-1}$  increased the  $T_g$  of about  $20^\circ\text{C}$  from ca.  $35^\circ\text{C}$  to  $55^\circ\text{C}$ . This is of importance since it allows to guaranty minimal mechanical properties changes of the high molecular weight thermoplastics in the eventuality of *in vivo* implantation.

### 3.2. Water uptake

Water uptake and weight loss of the copolymers were evaluated by weighing samples before and after degradation and were calculated from Eqs. (4) and (5). Results are shown in Fig. 2. Copolymers ( $200 \text{ kg}\cdot\text{mol}^{-1}$ ) presented low and stable water uptakes during the degradation with values under 10% even after 7 weeks. On the opposite,  $100 \text{ kg}\cdot\text{mol}^{-1}$  copolymers presented a higher absorption (up to 25% for 94T100) in agreement with their higher hydrophilicity resulting from a higher proportion of PEO blocks. As expected, crystallinity also influenced the water uptake, which increased up to 25% for the  $100\text{-kg}\cdot\text{mol}^{-1}$  samples with  $\text{PLA}_{94}$  blocks, whereas it remained stable and around 11% in the more crystalline  $\text{PLA}_{96}$  block copolymers.

### 3.3. Molecular weights and weight loss

Fig. 3 shows the evolution of  $M_n$  (measured by SEC) of the copolymers as a function of the degradation time.  $M_n$  decrease was observed for all copolymers with a faster average rate for  $100 \text{ kg}\cdot\text{mol}^{-1}$  copolymers, corresponding to 41% of the initial  $M_n$  compared to 22% for

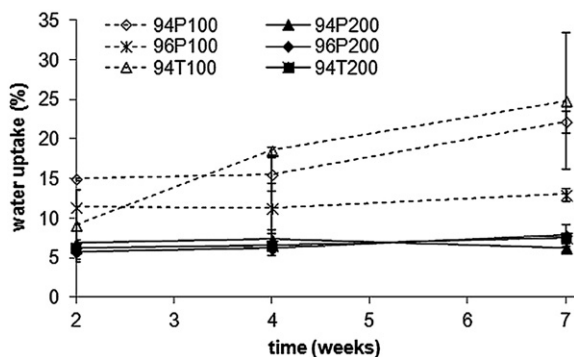


Fig. 2. Water uptake profiles of copolymers during degradation.

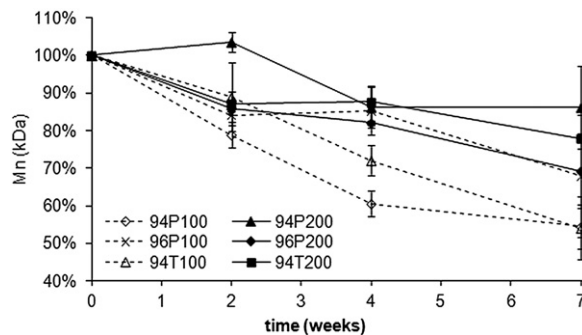


Fig. 3. Molecular weights of copolymers during degradation measured by SEC.

$200 \text{ kg}\cdot\text{mol}^{-1}$  copolymers at 7 weeks. It is to note that molecular weight distribution remained monomodal during the degradation with PD values in the range 1.5 to 2.0, which corresponds to a typical first step of hydrolytic degradation for this kind of PLA-based copolymers [30,31]. The higher degradation rates of the  $100\text{-kg}\cdot\text{mol}^{-1}$  copolymers compared to the  $200\text{-kg}\cdot\text{mol}^{-1}$  ones can be attributed to the EO/LA ratio. In agreement with what was observed for the water uptake, the more hydrophilic  $100 \text{ kg}\cdot\text{mol}^{-1}$  copolymers chains soak water more easily, which makes PLA chain hydrolysis faster. In addition, for the  $100\text{-kg}\cdot\text{mol}^{-1}$  copolymers, it was again found that crystallinity had an influence since the more crystalline 96P100 copolymer degraded more slowly than 94P100 copolymer. On the opposite, no influence of the central Pluronic and Tetric blocks was found. Finally, regarding the weight loss, they were similar for all samples and limited to a maximum of 5% during the 7-week degradation (data not shown). Again, this is in agreement with the degradation behavior of aliphatic polyesters where weight loss is limited during the early stages of degradation as a consequence of the impossibility for the degraded chains to diffuse out of the samples [23,30,32].

### 3.4. Thermal properties

Thermal properties were investigated by DSC during the degradation. Thermograms were plotted at various degradation times as exemplified for copolymer 96P200 (Fig. 4). All copolymers showed the same typical evolution. A first noticeable sign of degradation was the appearance of a cold crystallization peak around  $120^\circ\text{C}$  after only 2 weeks. With increasing degradation time, this peak became larger and the cold crystallization temperature ( $T_c$ ) decreased to about  $110^\circ\text{C}$ . Regarding the melting temperature, a broadening of the melting peak, located in the range  $140$  to  $160^\circ\text{C}$  depending on the copolymer, was observed as the degradation time increased. This was accompanied by the appearance of a second melting peak  $10^\circ\text{C}$  below the main peak. All these phenomena can be explained by the degradation and shortening of PLA chains. Shorter PLA chains have an increased mobility and are

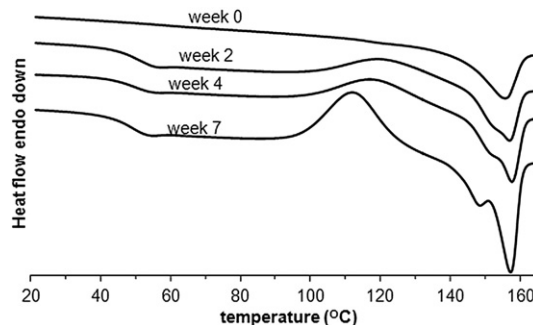


Fig. 4. Thermograms of the copolymer 96P200 during degradation (2nd heating ramp).

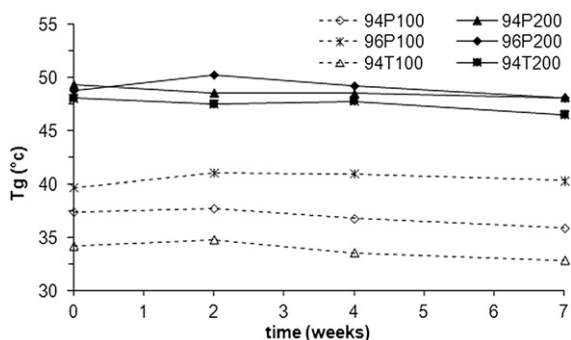


Fig. 5.  $T_g$  as a function of degradation time.

thus able to cold crystallize in multiple crystalline structures with different  $T_m$  [33,34].

As illustrated in Figs. 4 and 5, degradation did not lead to significant changes of  $T_g$  during the 7 weeks of degradation. More interestingly, and in agreement with the initial  $T_g$  values already discussed, it is important to note that  $200\text{-kg}\cdot\text{mol}^{-1}$  copolymers have a higher  $T_g$  (in the range  $47\text{--}50\text{ }^\circ\text{C}$ ) as a consequence of their high molecular weight, whereas  $100\text{ kg}\cdot\text{mol}^{-1}$  copolymers have  $T_g$  between  $30$  and  $41\text{ }^\circ\text{C}$ . Since glass transition may induce major changes in the mechanical behavior of semi-crystalline thermoplastic polymers, it is required for biomedical applications to work with polymers that do not have  $T_g$  in the range of physiological body temperature. As a consequence,  $100\text{ kg}\cdot\text{mol}^{-1}$

copolymers may not be used as implantable biomaterials whereas  $200\text{ kg}\cdot\text{mol}^{-1}$  copolymers could be further considered for such applications.

### 3.5. Mechanical properties

Each biological tissue has specific mechanical properties adapted to its function. Consequently, polymers for temporary biomedical applications have to mimic the mechanical behavior of the tissues they are supposed to replace as long as it is necessary, i.e., until tissues repair. For this reason, we were interested in evaluating the main tensile mechanical properties of our copolymers during the degradation process. Fig. 6(a) shows a typical stress-strain curve for our copolymers. This plot can be divided into three distinctive parts: the linear elastic region in which the material holds Hooke's law of elasticity ( $\sigma = \varepsilon E$ ) followed by, after the yield point, a decrease in the slope which corresponds to irreversible plastic deformation leading to the final damage and failure step. This profile is characteristic of ductile thermoplastic polymers and not of thermoplastic elastomers.

All other graphs in Fig. 6 show the evolution of the main tensile mechanical properties for the  $200\text{-kg}\cdot\text{mol}^{-1}$  copolymers over the degradation period. Profiles of the  $100\text{-kg}\cdot\text{mol}^{-1}$  copolymers are not presented here because their faster degradation induced so dramatic losses of their mechanical properties that many of them could not even be placed in the tensiometer grips without breaking. Results observed for the few samples that could have been analyzed were much lower than the  $200\text{-kg}\cdot\text{mol}^{-1}$  copolymers. Concerning 94P200, 96P200 and 94 T200, all mechanical properties ( $E$ ,  $\sigma_y$ ,  $\varepsilon_y$  and  $\sigma_f$ ) except  $\varepsilon_f$  remained in the same ranges during

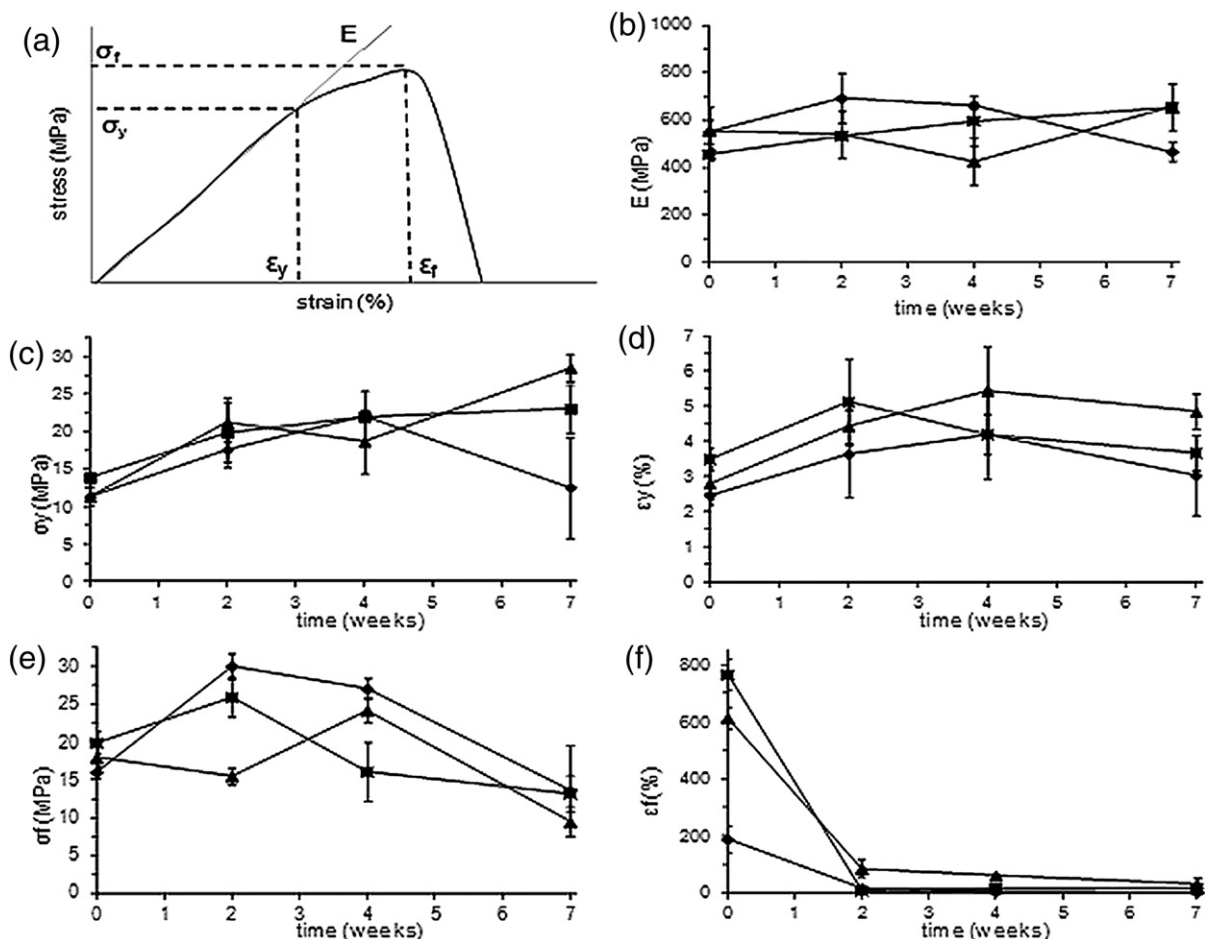


Fig. 6. Evolution of copolymers mechanical properties during degradation. (a) Representation of a typical tensile stress-strain curve obtained for a copolymer. (b) Young's modulus  $E$ . (c) yield stress  $\sigma_y$ . (d) yield strain  $\varepsilon_y$ . (e) Stress at failure  $\sigma_f$ . (f) Strain at  $\varepsilon_f$  failure.

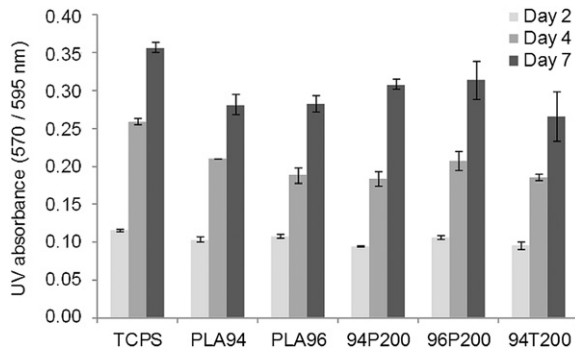


Fig. 7. *In vitro* proliferation of C3 cells on different polymers.

degradation (Fig. 6) with starting values of ca. 10 MPa for  $\sigma_y$ , ca. 2.5–3.5% for  $\epsilon_y$  and ca. 20 MPa for  $\sigma_f$ . However, small differences can be found. Indeed, while Young's modulus remained stable in the range 400 to 600 MPa for all copolymers, a common trend seemed to appear for the stress at failure ( $\sigma_f$ ), the yield stress ( $\sigma_y$ ) and the yield strain ( $\epsilon_y$ ). In a first step, up to 2 to 4 weeks of degradation, they slightly increased as a result of the initial preferable degradation of the amorphous domains resulting in an increase of crystallinity. This increase is well known for PLA and has been extensively studied by our group in the past [35]. After this initial period, mechanical properties decreased as a result of the polymer chains hydrolysis. In this second period, the decrease of molecular weight (see section 3.3) becomes the main parameter controlling mechanical properties. We can assume that all these properties would steadily decrease until the end of the degradation process.

In opposition to the slow evolution of the other mechanical properties, the strain at failure ( $\epsilon_f$ ; Fig. 6f) drastically decreased right from the beginning of degradation study for all copolymers that from a ductile behavior turned to a brittle one. This reveals a very strong impact of the chain scission and of the crystallinity increase on this property. It is of importance to note that this decrease corresponded to a drop of  $\epsilon_f$  by a factor 20 to 50 depending on the copolymer. In addition, while no difference could be found between the three copolymers in the evolution of the other properties, this is not the case for  $\epsilon_f$ . Indeed, the initial strain at failure was higher in the less crystalline 94P200 and 94 T200 copolymers ( $\epsilon_f \approx 600\text{--}700\%$ ) compared to the more crystalline 96P200 copolymer ( $\epsilon_f \approx 200\%$ ).

### 3.6. Cytocompatibility

The copolymers have been designed with the FDA approved Pluronic F127 [36] and PLA and the cytocompatible Tetronic 1107 [37]. In addition, to guaranty the overall bioresorbability of the copolymers, the non-degradable central blocks were chosen with molecular weights compatible with renal excretion. To confirm the expected cytocompatibility of the copolymers, the viability and the proliferation of C3 MSCs were tested by seeding the cells at the surface of polymer disks and assessed during a 7-day period. The behavior of the cells on the copolymers was compared to their behavior when cultured on TCPS and 200 kg·mol<sup>-1</sup> PLA homopolymer (PLA<sub>94</sub> and PLA<sub>96</sub>) control samples previously prepared in our laboratory. As shown in Fig. 7, similar level of cell viability was observed for all copolymers with no statistical differences in cell number cultured on copolymers, TCPS or control homopolymers after 7 days. Interestingly, the cells proliferated on the polymer samples with kinetics similar to that observed for cells cultured on TCPS. Cytocompatibility was confirmed with live/dead assay

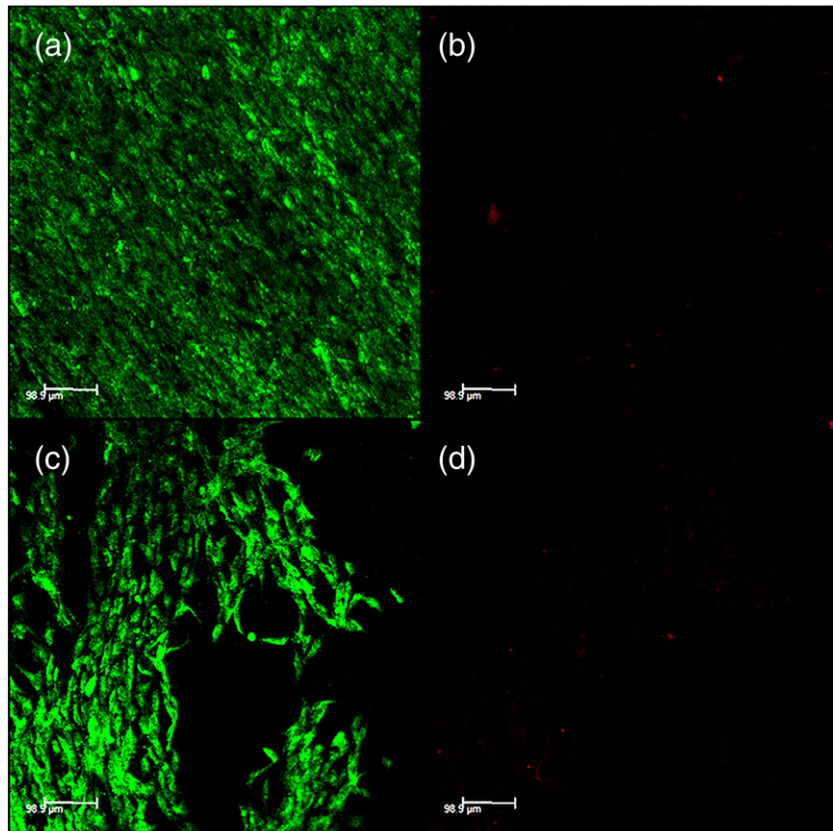


Fig. 8. Live/dead assay fluorescent microscopy pictures after 7 days of proliferation of C3 cells on 94P200 (a, b) and 94 T200 (c, d) copolymers. Staining highlights viable cells in green (a, c) and dead cells in red (b, d).

and confocal microscopy. Fig. 8a shows that C3 cells proliferated and entirely covered the surface of the copolymer. Moreover, almost no red staining was observed in Fig. 8b, indicating no cytotoxic effect on cells. Fig. 8c even shows elongated green C3 cells with a typical fibroblast-like morphology. The results not only confirmed that the copolymers are cytocompatible but also demonstrated that they allow both cell proliferation with normal morphology and high metabolic activity, which will be of benefit for future biomedical applications.

#### 4. Conclusion

In an attempt to develop new degradable biomaterials with specific mechanical properties, and in particular with high Young's moduli, we investigated the synthesis and the short-term degradation properties of PLA-based block copolymers containing Pluronic F127 and Tetronic 1107. This study showed the possibility of modulating the different degradation properties by changing the crystallinity of PLA blocks and the initial global molecular weight. 100 kg·mol<sup>-1</sup> copolymers suffered very important changes during hydrolytic degradation, illustrated by an early water uptake, a rapid molecular weight decrease and a total loss of mechanical properties after 7 weeks. These results, as well as DSC thermograms showing  $T_g$  close to the human body temperature, make them inappropriate for biomedical applications when mechanical stability is needed. On the opposite, even though 200 kg·mol<sup>-1</sup> copolymers showed a significant molecular weight decrease during degradation, they kept a higher mechanical integrity with maintained Young's moduli in the range 400 to 600 MPa. Due to their higher crystallinity, the copolymers based on PLA<sub>96</sub> also exhibited slightly lower strains at failure than those containing PLA<sub>94</sub>. Degradation rates associated with good cytocompatibility make the 200-kg·mol<sup>-1</sup> star and linear PLA copolymers interesting as materials for temporary biomedical applications requiring cell culture.

#### Acknowledgements

The authors thank the French Ministry of Education and Research for Adrien Leroy's fellowship.

#### References

- [1] S. Lyu, D. Untereker, *Int. J. Mol. Sci.* 10 (2009) 4033–4065.
- [2] M. Biondi, F. Ungaro, F. Quaglia, P.A. Netti, *Adv. Drug Deliv. Rev.* 60 (2008) 229–242.
- [3] S.M. Janib, A.S. Moses, J.A. MacKay, *Adv. Drug Deliv. Rev.* 62 (2010) 1052–1063.
- [4] J.D. Kretlow, L. Klouda, A.G. Mikos, *Adv. Drug Deliv. Rev.* 59 (2007) 263–273.
- [5] B. Dhandayuthapani, Y. Yoshida, T. Maekawa, D.S. Kumar, *Int. J. Polym. Sci.* 2011 (2011).
- [6] R. Langer, D.A. Tirrell, *Nature* 428 (2004) 487–492.
- [7] R. Langer, J.P. Vacanti, *Science* 260 (1993) 920–926.
- [8] B.-K. Chen, C.-H. Shen, S.-C. Chen, A.F. Chen, *Polymer* 51 (2010) 4667–4672.
- [9] T.A. Folliguet, C. Rücker-Martin, C. Pavoine, E. Deroubaix, M. Henaff, J.-J. Mercadier, S.N. Hatem, *J. Thorac. Cardiovasc. Surg.* 121 (2001) 510–519.
- [10] D.C. Surrao, S.D. Waldman, B.G. Amsden, *Acta Biomater.* 8 (2012) 3997–4006.
- [11] S.A. Guelcher, *Tissue Eng. B* 14 (2008) 3–17.
- [12] A. Harrane, A. Leroy, H. Nouailhas, X. Garric, J. Coudane, B. Nottelet, *Biomed. Mater.* 6 (2011).
- [13] Q. Liu, L. Jiang, R. Shi, L. Zhang, *Prog. Polym. Sci.* 37 (2012) 715–765.
- [14] M.C. Serrano, E.J. Chung, G.A. Ameer, *Adv. Funct. Mater.* 20 (2010) 192–208.
- [15] S.-I. Yang, Z.-H. Wu, W. Yang, M.-B. Yang, *Polym. Test.* 27 (2008) 957–963.
- [16] J. Fernández, A. Etxeberria, J.M. Ugarteandia, S. Petisco, J.-R. Sarasua, *J. Mech. Behav. Biomed. Mater.* 12 (2012) 29–38.
- [17] V.T. Lipik, J.F. Kong, S. Chattopadhyay, L.K. Widjaja, S.S. Liow, S.S. Venkatraman, M.J.M. Abadie, *Acta Biomater.* 6 (2010) 4261–4270.
- [18] I. Rashkov, N. Manolova, S.M. Li, J.L. Espartero, N. Manolova, M. Vert, *Macromolecules* 29 (1996) 50–56.
- [19] A.P. Pêgo, A.A. Poot, D.W. Grijpma, J. Feijen, *J. Control. Release* 87 (2003) 69–79.
- [20] Z. Zhang, D.W. Grijpma, J. Feijen, *J. Control. Release* 116 (2006) e29–e31.
- [21] D. Cohn, A. Hotovely-Salomon, *Polymer* 46 (2005) 2068–2075.
- [22] D. Cohn, A. Hotovely-Salomon, *Biomaterials* 26 (2005) 2297–2305.
- [23] S.M. Li, I. Rashkov, J.L. Espartero, N. Manolova, M. Vert, *Macromolecules* 29 (1996) 57–62.
- [24] M. Stefani, J. Coudane, M. Vert, *Polym. Degrad. Stab.* 91 (2006) 2853–2859.
- [25] H. Nouailhas, F. Li, A. El Ghzaoui, S. Li, J. Coudane, *Polym. Int.* 59 (2009) 1077–1083.
- [26] P. Aizawa, G. Karlsson, C. Benemar, V. Segl, K. Martinelle, E. Lindner, R. Smith, Effect of different materials used in bioreactor equipments on cell growth of human embryonic kidney (HEK293) cells cultivated in a protein-free medium cell technology for cell products, Springer, Netherlands, 2007. 459–462.
- [27] N. Blanchemain, T. Laurent, F. Chai, C. Neut, S. Haulon, V. Krump-konvalinkova, M. Morcellet, B. Martel, C.J. Kirkpatrick, H.F. Hildebrand, *Acta Biomater.* 4 (2008) 1725–1733.
- [28] M.-H. Huang, S. Li, M. Vert, *Polymer* 45 (2004) 8675–8681.
- [29] A. Kowalski, A. Duda, S. Penczek, *Macromolecules* 31 (1998) 2114–2122.
- [30] S.M. Li, H. Garreau, M. Vert, *J. Mater. Sci. Mater. Med.* 1 (1990) 123–130.
- [31] S.M. Li, H. Garreau, M. Vert, *J. Mater. Sci. Mater. Med.* 1 (1990) 131–139.
- [32] M. Hakkarainen, A.-C. Albertsson, S. Karlsson, *Polym. Degrad. Stab.* 52 (1996) 283–291.
- [33] L. Santonja-Blasco, R. Moriana, J.D. Badía, A. Ribes-Greus, *Polym. Degrad. Stab.* 95 (2010) 2185–2191.
- [34] S.S. Venkatraman, P. Jie, F. Min, B.Y.C. Freddy, G. Leong-Huat, *Int. J. Pharm.* 298 (2005) 219–232.
- [35] M. Vert, S. Li, H. Garreau, *J. Control. Release* 16 (1991) 15–26.
- [36] H.H. Jung, K. Park, D.K. Han, *J. Control. Release* 147 (2010) 84–91.
- [37] A. Rey-Rico, M. Silva, J. Couceiro, A. Concheiro, C. Alvarez-Lorenzo, *Eur. Cell. Mater.* 21 (2011) 317–340.